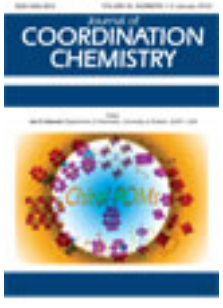

Journal of Coordination Chemistry
Publication details, including instructions for authors and subscription information:
http://www.tandfonline.com/loi/gcoo20

Indium(III) complexes containing bithiazole derivatives, chloride, methanol, and dimethyl sulfoxide: X-ray studies, spectroscopic characterization, and thermal analyses

Anita Abedi [a], Nasser Safari [b], Vahid Amani [b] & Hamid Reza Khavasi [b]

[a] Department of Chemistry, North Tehran Branch, Islamic Azad University, Tehran, Iran

[b] Department of Chemistry, Shahid Beheshti University, G. C., Evin, Tehran 983963113, Iran

Published online: 20 Jan 2012.

To cite this article: Anita Abedi, Nasser Safari, Vahid Amani & Hamid Reza Khavasi (2012) Indium(III) complexes containing bithiazole derivatives, chloride, methanol, and dimethyl sulfoxide: X-ray studies, spectroscopic characterization, and thermal analyses, Journal of Coordination Chemistry, 65:2, 325-338, DOI: 10.1080/00958972.2011.653638

To link to this article: http://dx.doi.org/10.1080/00958972.2011.653638

Journal of Coordination Chemistry
Vol. 65, No. 2, 20 January 2012, 325–338

Indium(III) complexes containing bithiazole derivatives, chloride, methanol, and dimethyl sulfoxide: X-ray studies, spectroscopic characterization, and thermal analyses

ANITA ABEDI†, NASSER SAFARI*‡, VAHID AMANI‡ and HAMID REZA KHAVASI‡

†Department of Chemistry, North Tehran Branch, Islamic Azad University, Tehran, Iran
‡Department of Chemistry, Shahid Beheshti University, G. C., Evin, Tehran 983963113, Iran

(*Received 3 October 2011; in final form 30 November 2011*)

[In(dm4bt)Cl_3(MeOH)] · 0.5dm4bt (**1**) (dm4bt is 2,2′-dimethyl-4,4′-bithiazole) and [In(4bt)Cl_3(MeOH)] (**2**) (4bt is 4,4′-bithiazole) were prepared from the reaction of 4,4′-bithiazole and 2,2′-dimethyl-4,4′-bithiazole with $InCl_3 \cdot 4H_2O$ in methanol, respectively. [In(4bt)Cl_3(DMSO)] (**3**) was also prepared from recrystallization of **2** in DMSO. These complexes were characterized by IR, UV-Vis, ^{1}H NMR, $^{13}C\{^1H\}$ NMR, and luminescence spectroscopy and their structures were studied by single-crystal X-ray crystallography. The thermal stabilities of **1** and **3** were studied by thermogravimetric and differential thermal analyses.

Keywords: Crystal structure; Indium(III) complexes; Thermogravimetric; Thermal analyses; Bithiazole derivative; Luminescence spectroscopy

1. Introduction

Indium compounds have applications in catalysis [1–4], electronics and optics [5, 6]. Transition metal complexes of bithiazole derivatives have found increasing applications. For example, Co(II) and Ni(II) complexes with 2,2′-diamino-4,4′-bithiazole (DABT) are effective inhibitors of DNA synthesis in tumor cells [7, 8], and multinuclear Fe(II) and Cu(II) complexes with a DABT Schiff base have been found to be excellent soft magnetic materials [9–12].

Several In^{III} complexes, [In(N–N)Cl_3(L)] (L = DMSO, H_2O, MeOH, and EtOH), are known, such as [In(bipy)Cl_3(H_2O)], [In(bipy)Cl_3(EtOH)], [In(bipy)Cl_3(H_2O)] · H_2O [13], [In(phen)Cl_3(DMSO)] [14], [In(4,4′-dmbpy)Cl_3(DMSO)] [15], [In(phen)Cl_3(H_2O)], [In(phen)Cl_3(EtOH)] · EtOH [16], and [In(5,5′-dmbpy)Cl_3(MeOH)] [17] (where bipy is 2,2′-bipyridine, phen is 1,10-phenanthroline, 5,5′-dmbpy is 5,5′-dimethyl-2,2′-bipyridine, and 4,4′-dmbpy is 4,4′-dimethyl-2,2′-bipyridine).

*Corresponding author. Email: n-safari@cc.sbu.ac.ir

ISSN 0095-8972 print/ISSN 1029-0389 online
http://dx.doi.org/10.1080/00958972.2011.653638

We recently reported coordination chemistry of 2,2′-dimethyl-4,4′-bithiazole (dm4bt) with Zn(II) and Hg(II) [18], Cd(II) [19], Tl(III) [20], Cu(II) [21], Fe(II) [22], and 4,4′-bithiazole (4bt) with Fe(II) [23]. Herein, the synthesis, characterization, and crystal structure of three new indium(III) complexes containing bithiazole ligands are reported.

2. Experimental

2.1. *Materials and physical methods*

All chemicals were purchased from Merck and Aldrich. Infrared (IR) spectra (4000–250 cm^{-1}) of solid samples were taken as 1% dispersion in CsI pellets using a Shimadzu-470 spectrometer. ^1H NMR spectra were recorded on a Bruker AC-300 spectrometer for protons at 300.13 MHz and for $^{13}C\{^1H\}$ NMR at 75.45 MHz in DMSO-d_6, and CD_3OD referred to TMS. Melting points were obtained by a Kofler Heizbank Rechart type 7841 melting point apparatus. Elemental analysis was performed using a Heraeus CHN-O Rapid analyzer, thermal behavior was measured with a STA 503 Bähr apparatus, UV-Vis spectra were recorded on a Shimadzu 2100 spectrometer using a 1 cm path length cell in CH_3OH and DMSO at room temperature, and luminescence spectra were recorded on a Perkin Elmer LS 45 using a 1 cm path length cell.

2.2. *Preparations*

2.2.1. Synthesis of [In(dm4bt)Cl_3(MeOH)] · 0.5dm4bt (1). 2,2′-Dimethyl-4,4′-bithiazole was prepared according to the literature [18]. 2,2′-Dimethyl-4,4′-bithiazole (0.20 g, 1.00 mmol) in methanol (15 mL) was added to a solution of $InCl_3 \cdot 4H_2O$ (0.15 g, 0.50 mmol) in methanol (15 mL) and the resulting colorless solution was stirred for 30 min at 45°C. This solution was left to evaporate slowly at room temperature. After 1 week, colorless prismatic crystals of **1** were isolated (yield: 0.21 g, 76.7%, m.p. 279–280°C). IR (CsI, cm^{-1}): 3427br, 3127m, 3083m, 2985w, 1518m, 1471m, 1431s, 1373m, 1298s, 1247m, 1214s, 1194m, 1165m, 1122w, 1091w, 1005s, 973m, 796s, 754s, 642w, 578w, 421m, 392m, 340m, 315m, 282m. UV-Vis: λ_{max} (MeOH, nm), 218 and 258. ^1H NMR (CD_3OD) (ppm): 2.79 (s, 3H), 3.40 (s, 1.5H), 7.75 (s, 1H), and 8.20 (s, 0.5 H). Anal. Calcd: C, 28.51; H, 2.92; N, 7.67. Found: C, 28.23; H, 2.89; N, 7.62.

2.2.2. Synthesis of [In(4bt)Cl_3(MeOH)] (2). 4,4′-Bithiazole was prepared according to the literature [24]. 4,4′-Bithiazole (0.17 g, 1.00 mmol) in methanol (15 mL) was added to a solution of $InCl_3 \cdot 4H_2O$ (0.15 g, 0.50 mmol) in methanol (15 mL) and the resulting colorless solution was stirred for 30 min at 45°C. This solution was left to evaporate slowly at room temperature. After 1 week, colorless prismatic crystals of **2** were isolated (yield: 0.17 g, 80.7%, m.p. > 300°C). IR (CsI, cm^{-1}): 3426br, 3079m, 2920m, 1634s, 1510s, 1431s, 1373m, 1317s, 1285m, 1157w, 1125w, 1060m, 1007m, 973s, 902s, 883m, 833s, 769m, 643m, 532w, 472m, 418m, 397m, 345m, 308m, 275m. UV-Vis: λ_{max} (MeOH, nm), 249. ^1H NMR (CD_3OD) (ppm): 8.51 (s, 1H) and 9.63 (s, 1H). Anal. Calcd: C, 19.95; H, 1.90; N, 6.64. Found: C, 19.82; H, 1.88; N, 6.59.

2.2.3. Synthesis of [In(4bt)Cl_3(DMSO)] (3). [In(4bt)Cl_3(MeOH)] (**2**) (0.18 g, 0.43 mmol) was dissolved in DMSO (5 mL) and the resulting pale yellow solution was stirred for 45 min at 60°C. This solution was left to evaporate slowly at room temperature. After 3 weeks, pale yellow prismatic crystals of **3** were isolated (yield: 0.14 g, 69.6%, m.p. > 300°C). IR (CsI, cm^{-1}): 3085m, 2999m, 2913w, 1555w, 1510s, 1432s, 1372w, 1318s, 1199w, 1158m, 1059m, 1023s, 994s, 970s, 946s, 907m, 881m, 830s, 775m, 715w, 642w, 475w, 438m, 395m, 343m, 310m, 266m. UV-Vis: λ_{max} (DMSO, nm), 265. ^{1}H NMR (DMSO-d_6): 8.07 (s, 1H) and 9.21 (s, 1H) ppm. $^{13}C\{^1H\}$ NMR (DMSO-d_6) (ppm): 116.3 (s), 151.3 (s), 155.7 (s). Anal. Calcd: C, 20.55; H, 2.14; N, 6.00. Found: C, 20.28; H, 2.11; N, 5.94.

2.3. *X-ray structure analysis*

The X-ray diffraction measurements were made on a Bruker SMART 1000 CCD area detector diffractometer at 100 K for **1** and **3** and a STOE IPDS IIT area detector diffractometer at 298 K for **2** (Mo-Kα radiation, graphite monochromator, $\lambda = 0.71073$ Å). The structures of **1**, **2**, and **3** were solved by SHELX-97 and SHELXTL ver. 5.1 and absorption corrections were done using the SADABS, X-Area 1.31, and APEX2 programs for **1**, **2**, and **3**, respectively [25–27]. Data collection, cell refinement, and data reduction were done by X-Area 1.31 and APEX2, SAINT, SHELXTL ver. 5.1, PLATON, and MERCURY [25–29].

3. Results and discussion

3.1. *Synthesis of 1, 2, and 3*

Complexes **1** and **2** were obtained by the reaction of one equivalent of $InCl_3 \cdot 4H_2O$ with two equivalents of the appropriate bithiazole in methanol at 45°C after 30 min, isolated in 76.7% and 80.7% yields, respectively. Complex **3** was obtained by recrystallization of **2** in DMSO. After recrystallization of **1** in DMSO, [In$(DMSO)_3Cl_3$] was formed, which had been previously fully characterized by X-ray analysis [30]. The synthetic routes of these complexes are shown in scheme 1.

3.2. *Spectroscopic characterization of 1, 2, and 3*

IR absorptions of **1**, **2**, and **3**, listed in the section 2, contain several bands from 600 to 3130 cm^{-1}, which are related to the hetero aromatic ring modes C–H, C=C, C=N, C–C, C–N, and S–C [13, 31, 32]. These bands for the free ligand are shifted to higher frequencies upon coordination in **1**, **2**, and **3** [13, 33–36]. This shift to higher frequencies upon coordination has been observed for bipyridine and 2,2′-dimethyl-4,4′-bithiazole ligands coordinated to metals as well [13, 33–36], and can be explained by changing the geometry of the free ligand from syn to anti orientation. The bands near 3060 cm^{-1} can be assigned to ν(C–H_{cycle}) for **1**, **2**, and **3** and bands near 2900 cm^{-1} can be assigned to ν(C–H_{Me}). Bands near 3325 cm^{-1} can be assigned to ν(O–H) for **1** and **2**. The new signal at 946 cm^{-1} in IR spectra of **3** has been assigned to ν(S=O) [37]. Far IR spectra of **1**, **2**,

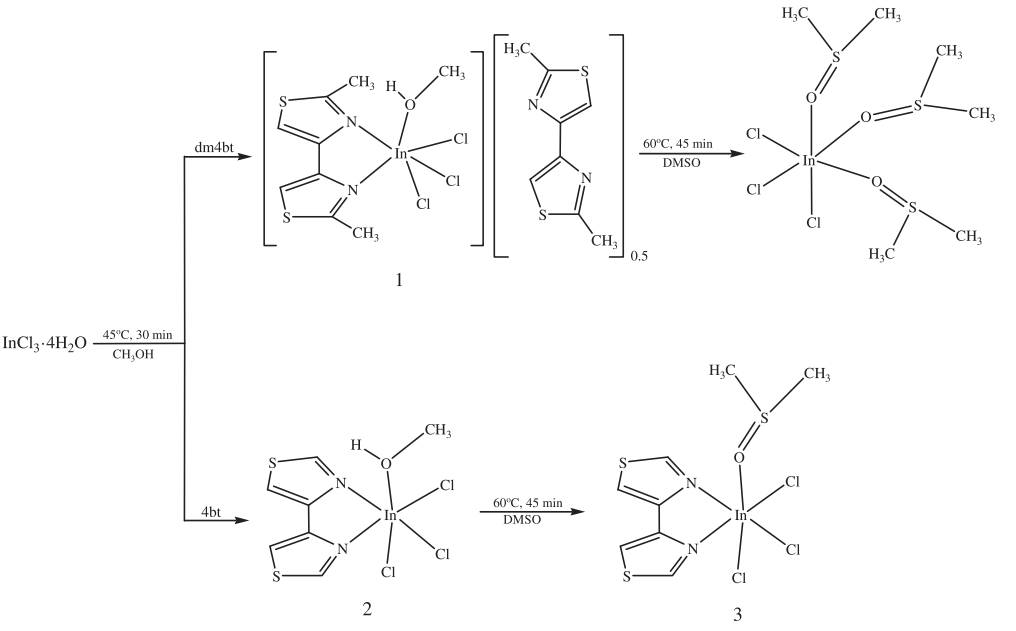

Scheme 1. The preparation methods of **1**, **2**, and **3**.

and **3** were recorded between 500 and 260 cm^{-1}. In–O stretching vibrations for **1**, **2**, and **3** are at 421, 418, and 438 cm^{-1} [38]. The In–N stretching vibration for **1** is at 392 and 340 cm^{-1}; for **2** it is at 397 and 345 cm^{-1} and for **3** at 395 and 343 cm^{-1}. In–Cl frequencies are at 315 and 282 cm^{-1} for **1**, at 308 and 275 cm^{-1} for **2** and 310 and 266 cm^{-1} for **3**, as expected [30, 39, 40].

The UV-Vis spectra of methanol solutions of **1** and **2** have bands at 218 and 258 nm for **1** and 249 nm for **2**; the DMSO solution of **3** has a band at 265 nm assigned to $\pi \rightarrow {}^{*}\pi$.

The ^{1}H NMR spectrum of **1** exhibited two sharp singlets at 2.79 and 3.40 ppm for CH_3 with intensity ratio of 2 : 1 owing to uncoordinated and coordinated dm4bt, respectively. Two sharp singlets at 7.75 and 8.20 ppm are also seen for CH of the ligand [18]. Coordination of dm4bt to In(III) results in shielding of the coordinated dm4bt compared to that of the uncoordinated. The bithiazole protons for **2** and **3** exhibit two sharp singlets at 8.51 and 9.63 ppm and 8.07 and 9.21 ppm for CH protons, respectively. The $^{13}C\{^{1}H\}$ NMR spectrum of **3** shows three singlets at 116.3, 151.2, and 155.7 ppm, as expected.

Luminescence emission spectra of bithiazole derivatives and **1**–**3** are displayed in figure 1. The dm4bt exhibits a weak broad luminescent emission centered at 453 nm and **1** displays two weak luminescent emissions at 328 and 454 nm. The band at 454 nm is related to uncoordinated ligand in **1**. There are blue-shifts of the emission energies of dm4bt after coordination to In(III) for **1** (125 nm blue-shifted compared to the related emission band). As shown in figure 1(b), the maximum emission of 4bt is at 371 nm. There are blue-shifts of the emission energies of 4bt after coordination to In(III) for **2** (41 nm blue-shift compared to the related emission band). This band in **2** is stronger than the band seen for the related ligand. As shown in figure 1(c), the maximum

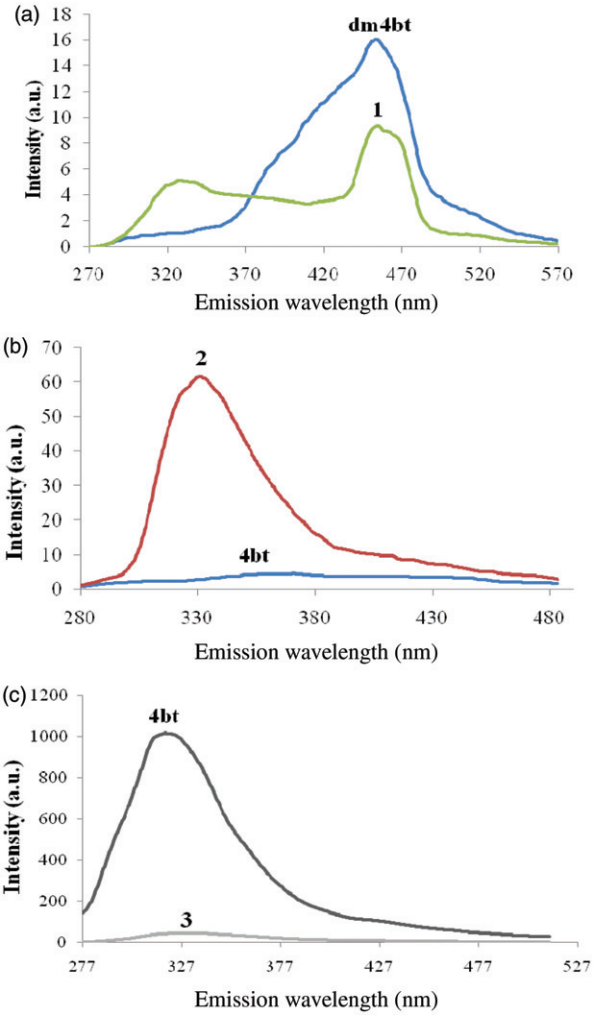

Figure 1. The luminescence spectra of (a) **dm4bt** (2.26×10^{-3} mol L^{-1}) and **1** (2.21×10^{-3} mol L^{-1}) in CH_3OH at room temperature; excitation wavelength = 258 nm. (b) **4bt** (2.81×10^{-3} mol L^{-1}) and **2** (2.83×10^{-3} mol L^{-1}) in CH_3OH at room temperature; excitation wavelength = 249 nm. (c) **4bt** (2.82×10^{-3} mol L^{-1}) and **3** (2.79×10^{-3} mol L^{-1}) in DMSO at room temperature; excitation wavelength = 265 nm.

emission of 4bt appeared at 319 nm, which is red-shifted after coordination to In(III) for **3** (9 nm red-shift compared to the related emission band). However, intensity of the emission band in **3** is weaker than the band for the free ligand. The shapes of the luminescence emission spectra for dm4bt, 4bt, **1**, **2**, and **3** are similar, so the emission properties of these compounds are believed to have originated from $\pi^* \rightarrow \pi$ transitions [41, 42]. Intensity of the signal in **2** increases. The luminescence of the ligand decreases in methanol by energy transfer *via* hydrogen-bonding, but this energy transfer process is reduced in **3**. In DMSO solution of **3**, the emission intensity of the complex is reduced compared to that of the free ligand by energy transfer.

3.3. *Thermal studies of 1 and 3*

The thermal stabilities of [In(dm4bt)Cl_3(MeOH)]·0.5dm4bt (**1**) and [In(4bt)Cl_3(DMSO)] (**3**) have been determined on single-crystal samples between 30°C and 500°C in air with a heating rate of 10°C min^{-1} by thermogravimetric (TG) and differential thermal analyses (DTA) (Supplementary material). For **1**, TGA shows that decomposition starts at 135°C and ends at 188°C with weight loss of 2.80%, equivalent to one methyl from methanol and the remaining weight corresponds to [In(dm4bt)Cl_3(OH)]·0.5dm4bt (**1**). Removal of non-coordinated dm4bt starts at 243°C and ends at 262°C with weight loss of 17.9%. Weight loss of 19.7% from 265°C to 490°C corresponds to removal of three chlorines and one hydrogen molecule with the remaining weight corresponding to [In(dm4bt)(O)]. Coordinated dm4bt is stable until 490°C where chlorine is lost. The DTA curve of **1** displays distinct endothermic peaks at 173°C, 179°C, 248°C, 280°C, and 438°C. For **3**, the weight loss of 16.28% from 185°C to 300°C corresponds to removal of DMSO and weight loss of 21.17% from 360°C to 500°C corresponds to removal of three Cl with the remaining weight corresponding to [In(4bt)]. The DTA curve of **3** displays two distinct endothermic peaks at 233°C and 377°C and two distinct exothermic peaks at 451°C and 474°C.

3.4. *Description of the molecular structures of 1, 2, and 3*

Crystallographic data for **1**, **2**, and **3** are given in table 1 and selected bond lengths and angles are presented in table 2. As shown in figure 2, the asymmetric unit of **1** contains one independent [In(dm4bt)(MeOH)Cl_3] and half dm4bt. In^{III} is six-coordinate in a distorted octahedral configuration by two nitrogen atoms from chelating 2,2′-dimethyl-4,4′-bithiazole, one methanol, and three Cl^-. The In–N bond lengths are 2.2959(11) and 2.3294(11) Å, In–Cl bond lengths are 2.4204(5) to 2.4483(4) Å and In–O bond length is 2.2854(10) Å (table 2). The N1–In–O1, N2–In–O1, Cl1–In–O1, and Cl2–In–O1 bond angles are 81.01(4)°, 76.28(4)°, 86.01(3)°, and 85.72(3)°, respectively (table 2). The thiazole ring is distorted from planarity. Mean planes of rings A (N1/C2/S1/C3/C4), B (N2/C7/S2/C6/C5), and C (In1/N1/C4/C5/N2) make dihedral angles with each other, A/B = 10.71°, A/C = 10.07°, and B/C = 9.93°. This distortion from planarity is due to steric hindrance of the methyl. This distortion cooperates with strong intermolecular O–H···N hydrogen-bonding (1.87 Å). The Cl2–In–O1 and Cl1–In–O1 bond angles of 85.72(3) and 86.01(3) are larger than N1–In–O1 and N2–In–O1 bond angles of 81.01(4) and 76.28(4).

As shown in figure 3, [In(dm4bt)Cl_3(MeOH)] are linked by intermolecular non-classical C–H···Cl hydrogen bonds and S···Cl short interactions in the *b*-direction. These 1-D chains are further linked to generate 2-D sheets parallel to the *ab*-plane from one side by π–π interaction between adjacent thiazole rings, Cg2···Cg2^{i} [distance = 3.4572(9) Å, symmetry code: ^{i} $1-x,-y,-z$, where Cg2 is centroid of the ring (N1/C2/S1/C3/C4) and short S···Cl contacts (table 3)]. From the other side, non-coordinated dm4bt is a bridge to link adjacent chains by classical O–H···N and non-classical C–H···Cl hydrogen bonds (table 4). As shown in figure 4, these 2-D sheets are further linked by C–H···Cl and S···Cl interaction to the generated 3-D structure.

The ORTEP view with numbering scheme for **2** is shown in figure 5. In the crystal structure of **2**, In^{III} is six-coordinate in a distorted octahedral configuration by

Table 1. Crystallographic and structure refinement data for **1**–**3**.

	1	**2**	**3**
Empirical formula	$C_{13}H_{16}Cl_3InN_3OS_3$	$C_7H_8Cl_3InN_3OS_2$	$C_8H_{10}Cl_3InN_2OS_3$
Formula weight	547.64	421.46	467.53
Temperature (K)	100(2)	298(2)	100(2)
Wavelength λ (Å)	0.71073	0.71073	0.71073
Crystal system	Monoclinic	Monoclinic	Monoclinic
Space group	$P2_1/n$	$P2_1/n$	$P2_1/c$
Unit cell dimensions (Å, °)	8.9266(14)	6.7537(4)	12.5584(9)
a	8.9266(14)	6.7537(4)	12.5584(9)
b	14.162(2)	13.3856(7)	8.5000(6)
c	15.762(2)	15.1801(10)	14.7599(11)
β	94.612(2)	96.802(5)	79.029(13)
Volume (Å^3), *Z*	1986.2(5), 4	1362.66(14), 4	1575.3(2), 4
Calculated density (g cm^{-3})	1.831	2.054	1.971
Absorption coefficient (mm^{-1})	1.915	2.608	2.394
F(000)	1084	816	912
Crystal size (mm^3)	$0.20 \times 0.19 \times 0.15$	$0.50 \times 0.48 \times 0.35$	$0.16 \times 0.15 \times 0.11$
θ range for data collection (°)	1.94–30.51	2.70–29.18	2.76–29.00
Index ranges	$-12 \le h \le 12$; $-20 \le k \le 20$; $-22 \le l \le 22$	$-9 \le h \le 8$; $-18 \le k \le 18$; $-20 \le l \le 20$	$-17 \le h \le 17$; $-11 \le k \le 11$; $-20 \le l \le 20$
Data collected	26,380	15,023	18,170
Unique data (R_{int})	6058, (0.0267)	3658, (0.0864)	4180, (0.0271)
Parameters, restraints	220, 0	149, 0	165, 0
Goodness-of-fit on F^2 (S)	1.003	1.122	1.002
Final R_1, wR_2 (obs. data)	0.0180, 0.0427	0.0345, 0.0780	0.0254, 0.0590
Final R_1, wR_2 (all data)	0.0202, 0.0435	0.0407, 0.0806	0.0301, 0.0612
Largest difference peak and hole (e Å^{-3})	0.409 and −0.355	0.518 and −1.000	0.753 and −0.502

Table 2. Selected bond distances (Å) and angles (°) for **1**–**3**.

	1	**2**	**3**
In1–O1	2.2854(10)	2.304(2)	2.2186(18)
In1–N1	2.2959(11)	2.296(2)	2.305(2)
In1–N2	2.3294(11)	2.276(2)	2.267(2)
In1–Cl1	2.4483(4)	2.4100(9)	2.4492(6)
In1–Cl2	2.4413(4)	2.4031(9)	2.4450(6)
In1–Cl3	2.4204(5)	2.4952(8)	2.4438(7)
O1–In1–N1	81.01(4)	83.65(9)	81.08(7)
O1–In1–N2	76.28(4)	81.43(10)	80.37(7)
N1–In1–N2	73.07(4)	71.81(9)	72.38(7)
O1–In1–Cl3	169.59(3)	171.24(6)	171.37(5)
N1–In1–Cl3	94.51(3)	89.58(7)	92.06(5)
N2–In1–Cl3	93.45(3)	91.20(7)	92.61(6)
O1–In1–Cl2	85.72(3)	89.66(8)	88.49(5)
N1–In1–Cl2	91.93(3)	90.60(7)	91.75(5)
N2–In1–Cl2	158.02(3)	160.98(7)	161.76(6)
Cl2–In1–Cl3	103.899(13)	95.98(4)	96.99(2)
O1–In1–Cl1	86.01(3)	87.62(7)	89.21(5)
N1–In1–Cl1	165.99(3)	161.42(7)	162.72(5)
N2–In1–Cl1	98.79(3)	90.72(7)	92.00(6)
Cl1–In1–Cl3	97.394(14)	97.25(3)	96.08(2)
Cl1–In1–Cl2	92.345(16)	105.75(4)	102.31(2)

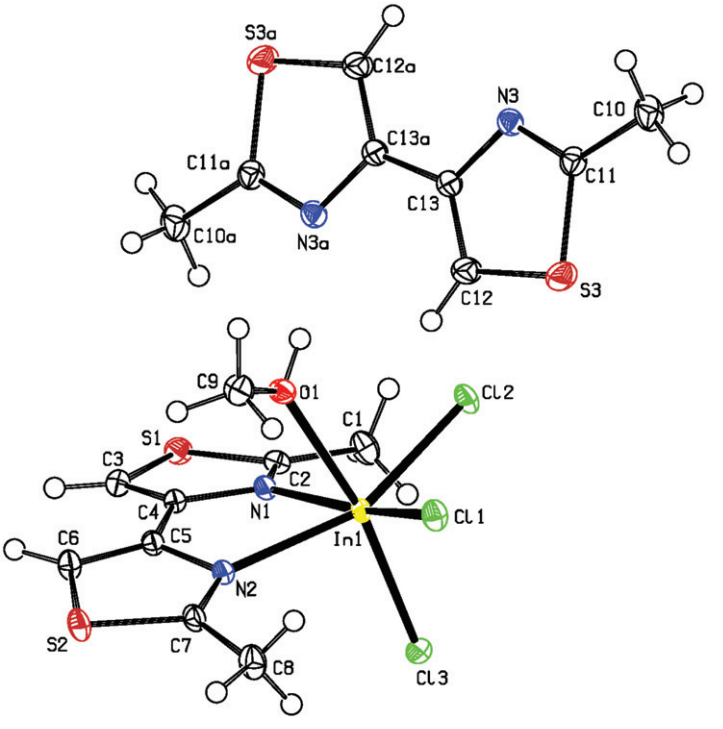

Figure 2. The labeling diagram of **1**. Thermal ellipsoids are at 30% probability; symmetry code: (a) $2-x, 1-y, -z$.

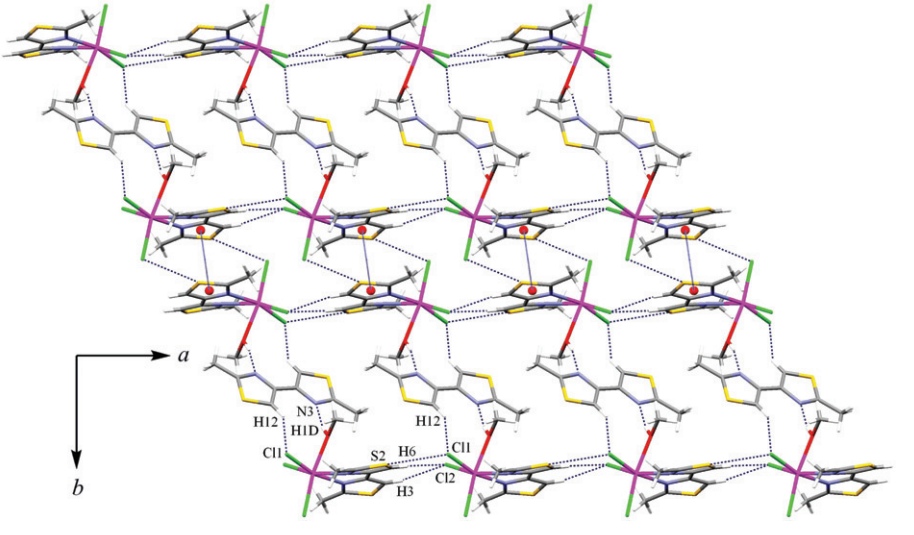

Figure 3. Intra and intermolecular O–H···N and C–H···Cl hydrogen bonds, short S···Cl contacts, and π–π interaction in **1** viewed along the *c*-axis. Hydrogen-bond distances: H12···Cl1 = 2.914, H1D···N3 = 1.870, H6···Cl2 = 2.810, H3···Cl2 = 2.700. S2···Cl1 contact is 3.5296(7) Å and Cg···Cg is 3.4572(9) Å.

Table 3. Selected bond distances S···Cl and S···S (Å) for **1–3**.

1			
Cl1···S1^{i}	3.4857(7)	Cl1···S2^{iii}	3.5296(7)
Cl3···S1^{ii}	3.4514(7)	S1···Cl1^{iv}	3.4857(7)
2			
S2···S1^{v}	3.5811(15)	Cl2···S1^{vii}	3.5617(14)
Cl1···S2^{vi}	3.3610(14)	Cl2···S2^{viii}	3.6772(15)
3			
Cl1···S3	3.4914(9)	Cl3···S1^{xi}	3.5039(10)
Cl2···S2^{ix}	3.5247(10)	S1···S2^{xii}	3.4315(10)
Cl2···S3	3.5222(9)	Cl2···S3^{x}	3.6147(9)

Symmetry codes: (i) $1/2+x, 1/2-y, 1/2+z$; (ii) $1-x, -y, -z$; (iii) $1+x, y, z$; (^{iv}) $-1/2+x, 1/2-y, -1/2+z$; (^{v}) $-x, -y, -z$; (^{vi}) $1/2+x, 1/2-y, 1/2+z$; (vii) $1/2+x, -1/2-y, 1/2+z$; (viii) $1/2-x, -1/2+y, 1/2-z$; (ix) $x, 1/2-y, -1/2+z$; (x) $-x, -y, -z$; (xi) $x, 1/2-y, -1/2+z$; $1/2-z$; (xii) $x, 3/2-y, 1/2+z$.

Table 4. Hydrogen-bond geometry for **1–3** in crystal packing (Å, °).

	D–H···A	D–H	H···A	D···A	D–H···A	Symmetry code
1	O1–H1D···N3	0.8500	1.8700	2.7002(16)	164.0	$2-x, 1-y, -z$
	C3–H3···Cl2	0.9500	2.7000	3.6397(15)	168.00	$-1+x, y, z$
	C6–H6···Cl2	0.9500	2.8100	3.7375(15)	167.00	$-1+x, y, z$
	C8–H8A···Cl1	0.9600	2.7700	3.5191(16)	136.00	–
	C8–H8C···Cl2	0.9600	2.7500	3.6420(16)	154.00	$-1/2+x, 1/2-y, -1/2+z$
	C9–H9B···Cl1	0.9800	2.8000	3.4660(16)	126.00	–
	C12–H12···Cl1	0.9500	2.9140	3.683(16)	138.85	–
2	O1–H1B···Cl3	0.73(4)	2.47(5)	3.202(3)	171(5)	$-1+x, y, z$
	C7–H7A···S1	0.96	2.97	3.587(4)	124	$-1/2-x, -1/2+y, 1/2-z$
	C7–H7B···S2	0.96	2.89	3.741(5)	148	$-1/2-x, -1/2+y, 1/2-z$
3	C7–H7B···Cl2	0.9800	2.7300	3.517(3)	137.00	$-x, -y, -z$
	C7–H7C···O1	0.9800	2.4000	3.378(3)	173.00	$-x, 1-y, -z$
	C2–H2···Cl3	0.9500	2.9000	3.436(3)	177.00	$1-x, 1-y, -z$
	C6–H6···Cl2	0.9500	2.9300	3.466(3)	177.00	$x, 1/2-y, 1/2+z$

two nitrogen atoms from chelating 4,4′-bithiazole, one methanol, and three Cl^{-}. The In–N bond lengths are 2.296(2) and 2.276(2) Å, In–Cl bond lengths are 2.4031(9) to 2.4952(8) Å and In–O bond length is 2.304(2) Å (table 2). The In–Cl, In–O, and In–N bond lengths and angles (table 2) are within normal range [19, 23]. The thiazole ring is slightly distorted from planarity. The mean planes of rings A (N1/C1/S1/C2/C3), B (N2/C6/S2/C5/C4), and C (In1/N1/C3/C4/N2) make the following dihedral angles, A/B = 2.42°, A/C = 2.93°, and B/C = 2.59°.

In the crystal structure of **2**, figure 6, π–π interaction between the thiazole rings, Cg2···Cg3^{i} [distance = 3.9314(17) Å, symmetry code: ^{i} $-x, -y, -z$, where Cg2 and Cg3 are centroids of the rings (N1/C1/S1/C2/C3) and (N2/C6/S2/C5/C4), respectively] along the *a*, *b*, and *c* axes, intermolecular C–H···Cl and C–H···S hydrogen bonds (table 4) along the *a*, *b*, and *c* axes, S···S interaction along the *a* and *b* axes and S···Cl interaction along the *a* and *b* axes (table 3) are effective in stabilization of the crystal structure and formation of the 3-D supramolecular complex.

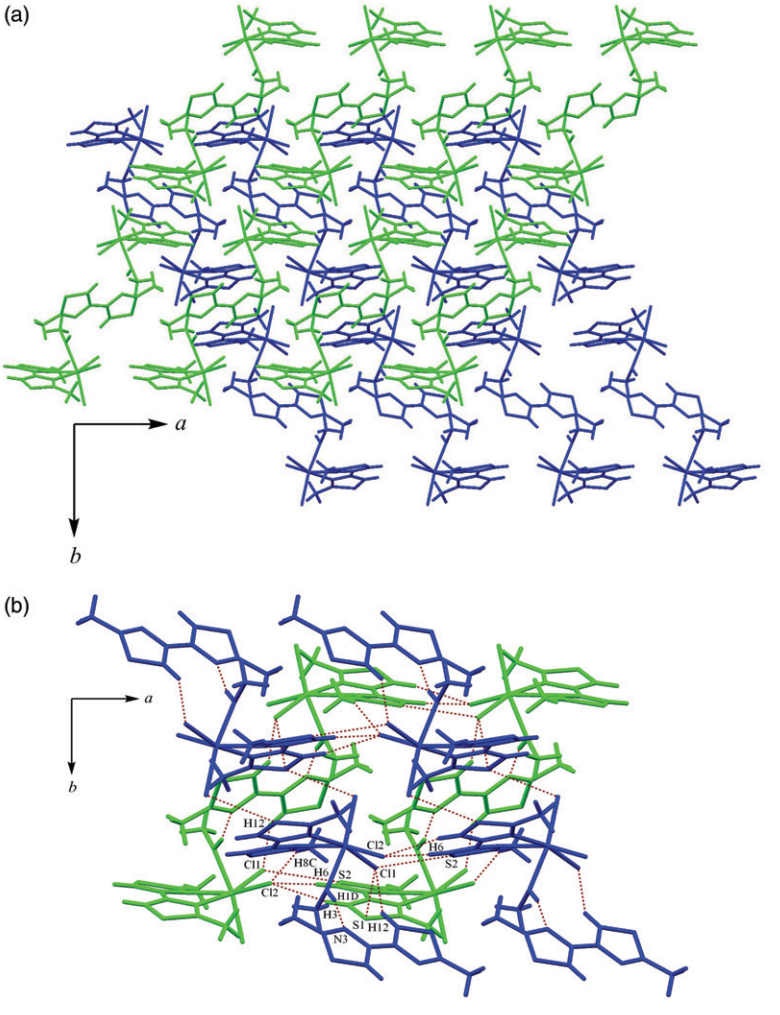

Figure 4. (a) Packing for **1** viewed along the *c*-axis. (b) Short S···Cl contacts and intermolecular O–H···N and C–H···Cl hydrogen bonds in **1** viewed along the *c*-axis. Hydrogen-bond distances: H12···Cl1 = 2.914, H1D···N3 = 1.870, H6···Cl2 = 2.810, H3···Cl2 = 2.700, H8C···Cl2 = 2.750. S1···Cl1 and S2···Cl1 contacts are 3.4857(7) and 3.5296(7) Å, respectively.

The ORTEP view with numbering scheme for **3** is shown in figure 7. In the crystal structures of **3**, In^{III} is six-coordinate in a distorted octahedral configuration by two nitrogen atoms from chelating 4,4′-bithiazole ligand, one oxygen atom from dimethyl sulfoxide, and three Cl^-. The In–N bond lengths are 2.305(2) and 2.267(2) Å, In–Cl bond lengths are 2.4438(7) to 2.4492(6) Å, and In–O bond length is 2.2186(18) Å (table 2). The In–Cl, In–O, and In–N bond lengths and angles (table 2) are within normal range [20, 21]. The thiazole ring is slightly distorted from planarity with mean planes of rings A (N1/C1/S1/C2/C3), B (N2/C6/S2/C5/C4), and C (In1/N1/C3/C4/N2) making the following dihedral angles, A/B = 1.69°, A/C = 1.38°, and B/C = 0.38°.

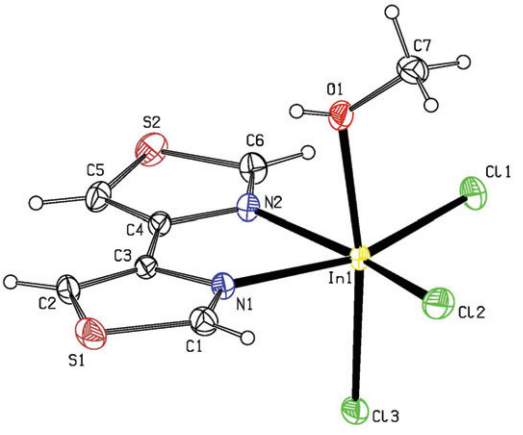

Figure 5. The labeling diagram of [In(4bt)Cl_3(MeOH)] (**2**). Thermal ellipsoids are at 30% probability.

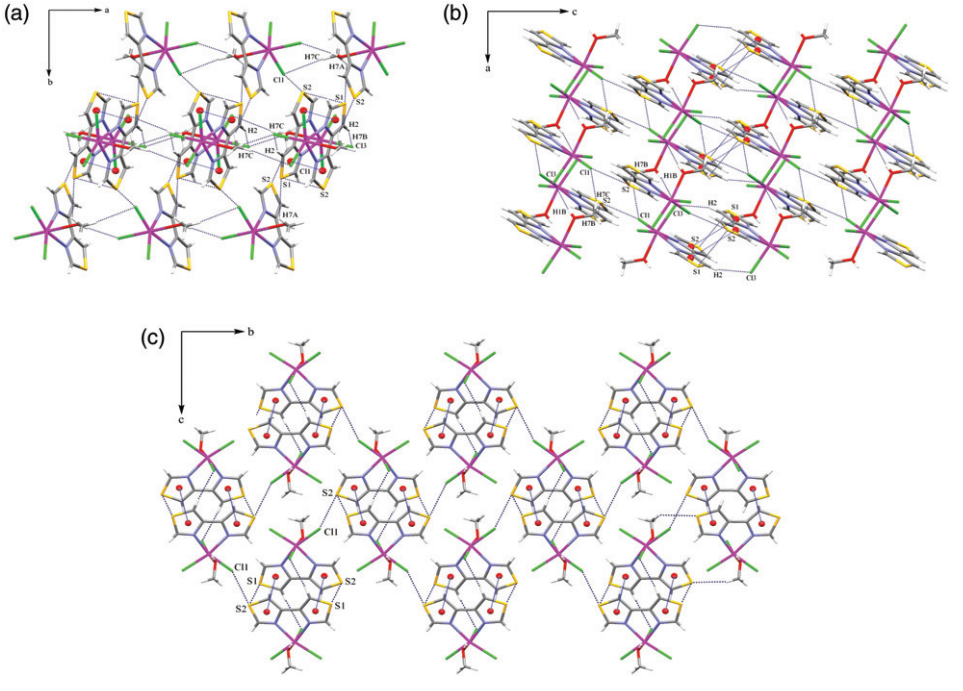

Figure 6. (a) Short S···Cl and S···S contacts, π–π interaction and intermolecular C–H···Cl and C–H···S hydrogen bonds in **2** viewed along the *c*-axis. (b) Short S···Cl and S···S contacts, π–π interaction and intermolecular C–H···Cl and C–H···S hydrogen bonds in **2** viewed along the *b*-axis. (c) Short S···S contacts, π–π interaction and intermolecular C–H···Cl and C–H···S hydrogen bonds in **2** viewed along the *a*-axis. Hydrogen-bond distances: H2···Cl3 = 2.844, H1B···Cl3 = 2.47(5), H7C···Cl = 2.848, H7B···S2 = 2.89, H7A···S1 = 2.97. S2···Cl1 and S1···S2 contacts are 3.3610(14) and 3.5811(15) Å, respectively, and Cg···Cg is 3.9314(17) Å.

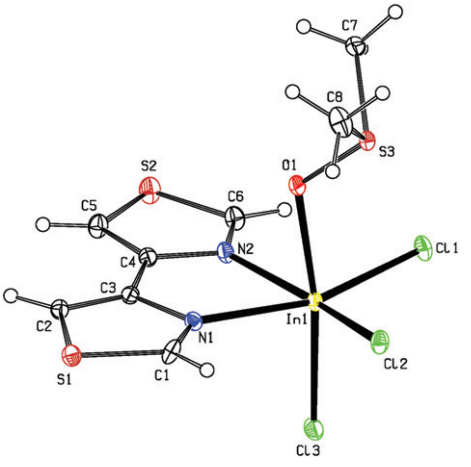

Figure 7. The labeling diagram of $[In(4bt)Cl_3(DMSO)]$ (**3**). Thermal ellipsoids are at 30% probability.

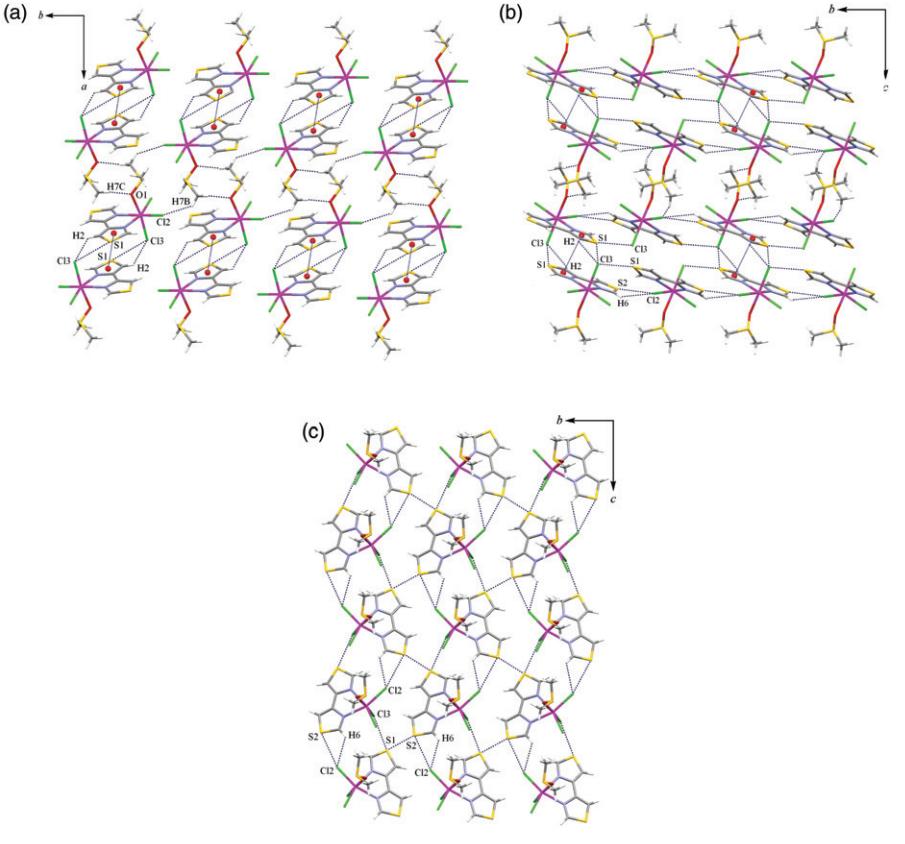

Figure 8. (a) Short S···Cl contacts, π–π interaction and intermolecular C–H···Cl hydrogen bonds in **2** viewed along the *c*-axis. (b) Short S···Cl contacts, π–π interaction and intermolecular C–H···Cl and C–H···Ohydrogen bonds in **2** viewed along the *b*-axis. (c) Short S···S and S···Cl contacts and intermolecular C–H···Cl hydrogen bonds in **2** viewed along the *a*-axis. Hydrogen-bond distances: H2···Cl3 = 2.900, H6···Cl2 = 2.930, H7C···O1 = 2.400, H7B···Cl2 = 2.730. S1···Cl3, S2···Cl2, and S1···S2 are 3.5039(10), 3.5247(10), and 3.4315(10) Å, respectively, and Cg···Cg is 3.5865(14) Å.

In the crystal structure of **3**, figure 8, the π–π interaction between the thiazole rings, Cg2 $\cdots$ Cg2^{i}, distance = 3.5865(14) Å, symmetry code: ^{i} $1-x, 1-y, -z$, where Cg2 is centroid of the ring (N1/C1/S1/C2/C3) along the *b* and *c* axes, intermolecular C–H $\cdots$ Cl and C–H $\cdots$ O hydrogen bonds (table 4) along the *a*, *b*, and *c* axes, S $\cdots$ S interaction along the *a*-axis and S $\cdots$ Cl interaction along the *a*, *b*, and *c* axes (table 3) are effective in stabilization of the crystal structure and formation of the 3-D supramolecular complex.

Supplementary material

CCDC Nos. 846066, 846067, and 846068 contain the supplementary crystallographic data for **1**, **2**, and **3**, respectively. These data can be obtained free of charge *via* http://www.ccdc.cam.ac.uk/conts/retrieving.html, or from the Cambridge Crystallographic Data Centre, 12 Union Road, Cambridge CB2 1EZ, UK; Fax: (+44) 1223 336 033; or E-mail: deposit@ccdc.cam.ac.uk

Acknowledgments

We thank the Graduate Study Councils of Islamic Azad University, North Tehran Branch and Shahid Beheshti University for the financial support.

References

[1] C.G. Frost, J.P. Hartley. *Mini-Rev. Org. Chem.*, **1**, 1 (2004).
[2] C.L. Allen, C. Burel, J.M.J. Williams. *Tetrahedron Lett.*, **51**, 2724 (2010).
[3] M.V. Nandakumar, A. Tschöp, H. Krautscheid, C. Schneider. *Chem. Commun.*, 2756 (2007).
[4] A. Wildermann, Y. Foricher, T. Netscher, W. Bonrath, *Pure Appl. Chem.*, **79**, 1839 (2007).
[5] C. Li, D. Zhang, S. Han, X. Liu, T. Tang, B. Lei, Z. Liu, C. Zhou. *Ann. N.Y. Acad. Sci.*, **1006**, 104 (2003).
[6] M.F. Cansizoglu, R. Engelken, H.W. Seo, T. Karabacak. *ACS Nano.*, **4**, 733 (2010).
[7] L.M. Fisher, R. Kuroda, T. Sakai. *Biochemistry*, **24**, 3199 (1985).
[8] M.J. Waring. *Ann. Rev. Biochem.*, **50**, 159 (1981).
[9] W. Sun, X. Gao, F. Lu. *J. Appl. Polym. Sci.*, **64**, 2309 (1997).
[10] J. Weng, W. Sun, L. Jiang, Z. Shen. *Macromol. Rapid Commun.*, **21**, 1099 (2000).
[11] L. Jiang, W. Sun. *Polym. Adv. Technol.*, **16**, 646 (2005).
[12] W. Sun, L. Jiang, J. Weng, B. He, Z. Shen. *Mater. Chem. Phys.*, **78**, 676 (2003).
[13] M.A. Malyarick, S.P. Petrosyants, A.B. Ilyukhin. *Polyhedron*, **11**, 1067 (1992).
[14] D. Nan, W. Naidong, D. Zhenchao, H. Shengzhi. *Jiegou Huaxue*, **6**, 145 (1987).
[15] R. Ahmadi, K. Kalateh, A. Abedi, V. Amani, H.R. Khavasi. *Acta Crystallogr.*, **E64**, m1306 (2008).
[16] A.B. Ilyukhin, M.A. Malyarik. *Kristallografiya*, **39**, 439 (1994).
[17] K. Kalateh, R. Ahmadi, A. Ebadi, V. Amani, H.R. Khavasi. *Acta Crystallogr.*, **E64**, m1353 (2008).
[18] H.R. Khavasi, A. Abedi, V. Amani, B. Notash, N. Safari. *Polyhedron*, **27**, 1848 (2008).
[19] B. Notash, N. Safari, A. Abedi, V. Amani, H.R. Khavasi. *J. Coord. Chem.*, **62**, 1638 (2009).
[20] B. Notash, N. Safari, H.R. Khavasi, V. Amani, A. Abedi. *J. Organomet. Chem.*, **693**, 3553 (2008).
[21] R. Al-Hashemi, N. Safari, A. Abedi, B. Notash, V. Amani, H.R. Khavasi. *J. Coord. Chem.*, **62**, 2909 (2009).
[22] A. Abedi, N. Safari, V. Amani, H.R. Khavasi. *Dalton Trans.*, **40**, 6877 (2011).
[23] A. Abedi, V. Amani, N. Safari. *Acta Crystallogr.*, **E67**, m311 (2011).
[24] H. Erlenmeyer, H. Ueberwasser. *Helv. Chim. Acta*, **22**, 938 (1939).

[25] G.M. Sheldrick. *SADABS*, Bruker AXS, Madison, WI, USA (1998).
[26] Stoe & Cie. *X-AREA (Version 1.31): Program for the Acquisition and Analysis of Data*, Stoe & Cie GmbH, Darmstadt, Germany (2009).
[27] Bruker. *APEX2 Software Package (Version 2.0-1)*, Bruker AXS Inc., Madison, WI, USA (2005).
[28] G.M. Sheldrick. *SHELXTL (Version 5.1), Structure Determination Software Suite*, Bruker AXS, Madison, WI, USA (1998).
[29] *Mercury 1.4.1*, Copyright Cambridge Crystallographic Data Center, 12 Union Road, Cambridge CB2 1EZ, UK (2001–2005).
[30] W.T. Robinson, C.J. Wilkins, Z. Zeying. *J. Chem. Soc., Dalton Trans.*, 219 (1990).
[31] M.G. Drew, T.R. Pearson, B.P. Murphy, S.M. Nelson. *Polyhedron*, **2**, 269 (1983).
[32] A. Morsali, M. Payheghader, M.R. Poorheravi, F. Jamali. *Z. Anorg. Allg. Chem.*, **629**, 1627 (2003).
[33] A. Neels, H.S. Evans. *Inorg. Chem.*, **38**, 6164 (1999).
[34] A.K. Boudalis, C.P. Raptopoulou, A. Terzis, S.P. Perlepes. *Polyhedron*, **23**, 1271 (2004).
[35] V. Amani, N. Safari, H.R. Khavasi. *Polyhedron*, **26**, 4257 (2007).
[36] V. Amani, N. Safari, H.R. Khavasi, P. Mirzaei. *Polyhedron*, **26**, 4908 (2007).
[37] K. Nakamoto. *Infrared and Raman Spectra of Inorganic and Coordination Compound Part B: Application in Coordination, Organometallic and Bioinorganic Chemistry*, John Wiley and Sons Inc., New York (2009).
[38] A.M. Abbassi, M. Skripkin, M. Kritikos, I. Persson, J. Mink, M. Sandström. *Dalton Trans.*, 1746 (2003).
[39] D.H. Brown, D.T. Stewart. *J. Inorg. Nucl. Chem.*, **32**, 3751 (1970).
[40] R.A. Walton. *J. Chem. Soc. A*, 1485 (1967).
[41] S.G. Liu, J.L. Zuo, Y.Z. Li, X.Z. You. *J. Mol. Struct.*, **705**, 153 (2004).
[42] C.K. Modi, D.H. Jani, H.S. Patel, H.M. Pandya. *Spectrochim. Acta A*, **75**, 1321 (2010).